K-quantum nonlinear coherent states: formulation, realization and nonclassical effects

Nguyen Ba An

National Center for Theoretical Sciences, P. O. Box 2-131, Hsinchu, Taiwan

300, R. O. C.

We introduce a generalized class of states called K-quantum nonlinear coherent states. Each K-state has K j-components corresponding to one and the same eigenvalue. Each Kj-component can be composed of K $K = 1$-states in a correlated manner. The introduced states are shown to be realized in the long-term behavior of the vibrational motion of an ion properly trapped and laser-driven. Nonclassical properties of the states are studied in detail.

PACS numbers: 42.50.Dv, 42.50.Vk, 32.80.Pj

I. INTRODUCTION

The coherent state (CS) introduced in 1963 [1,2] has become an useful and necessary tool to treat ideal boson fields subjected to external pumping sources. However, CS's cannot describe nonclassical effects such as antibunching, squeezing, etc. The conventional squeezed states [3] has been generalized to different types of higher-order ones [4–7], still for ideal bosonic particles. Elementary excitations in matter, on the other hand, are quasi-particles often obeying neither Bose-Einstein nor Fermi-Dirac statistics. Recently, the notion of nonlinear coherent state (NCS) has emerged to adequately deal with such quasi-particles with commutation relations deformed from the usual boson/fermion ones. q-deformed oscillators [8,9] were found as a particular case of the general f-oscillators [10] which possess in themselves a kinematic nonlinearity causing orbit-dependent oscillation frequencies. The NCS [11–15] is defined as the right-hand eigenstate $|\xi; f\rangle$ of the nonboson operator $A = af(\widehat{n})$,

$$A |\xi; f\rangle = \xi |\xi; f\rangle, \tag{1}$$

with $\widehat{n} = a^+ a$, a the bosonic annihilation operator, ξ a complex eigenvalue and f an arbitrary nonlinear operator-valued function of $\widehat{n}$. An island where NCS's find their life is single trapped ions driven by lasers [11,16–19].

In this paper we introduce the K-quantum nonlinear coherent state (KNCS) which reduces to the usual NCS defined by Eq. (1) when $K = 1$. In Section II the formulation is given for the KNCS together with their mathematical properties. Section III is devoted to a physical scheme of generation of KNCS's. Their nonclassical properties are studied in detail in Section IV. Conclusion is the final section.

II. K-QUANTUM NONLINEAR COHERENT STATES

The KNCS is a generalization of the NCS to the K right-hand eigenstates $|\xi; Kj, f\rangle$ of the non-Hermitian operator $a^K f(\widehat{n})$ as

$$a^K f(\widehat{n}) |\xi; Kj, f\rangle = \xi |\xi; Kj, f\rangle \tag{2}$$

where $K = 1, 2, ...$ and $j = 0, 1, ..., K - 1$. Spanned in the Fock basis $|n\rangle$,

$$|\xi; Kj, f\rangle = \sum_{n=0}^{\infty} c_n |n\rangle, \tag{3}$$

the expansion coefficients satisfy the recurrence equation

$$c_{m+K} = \frac{\xi \sqrt{m!}}{\sqrt{(m+K)!} f(m+K)} c_m. \tag{4}$$

Equation (4) determines all the c's if c_j with $j = 0, 1, ..., K - 1$ are known,

$$c_{nK+j} = \frac{\xi^n c_j}{\sqrt{(nK+j)!} f(nK+j)(!)^K}, \tag{5}$$

where

$$f(l)(!)^K \equiv \begin{cases} f(l)f(l-K)f(l-2K)...f(m) & \text{if } l \geq K \\ 1 & \text{if } 0 \leq l \leq K - 1 \end{cases}. \tag{6}$$

Of course, $0 \leq m \leq K - 1$, in Eq. (6). The c_j in Eq. (5) are themselves determined by the normalization condition $\langle \xi; Kj, f | \xi; Kj, f \rangle = 1$ which yields

$$c_j \rightarrow c_{Kj} \equiv c_{Kj}(|\xi|^2)$$
$$= \left[\sum_{m=0}^{\infty} \frac{|\xi|^{2m}}{(mK+j)! \left| f(mK+j)(!)^K \right|^2} \right]^{-1/2}. \tag{7}$$

In principle, the c_{Kj} is uncertain up to a phase factor. In Eq. (7) we have chosen the phase such that the usual CS results in the limit $f \equiv 1$ and $K = 1$. The explicit form of the KNCS is then

$$|\xi; Kj, f\rangle = c_{Kj} \sum_{n=0}^{\infty} \frac{\xi^n}{\sqrt{(nK+j)!} f(nK+j)(!)^K} |nK+j\rangle. \tag{8}$$

Unlike the usual CS whose eigenvalues spread the whole complex plane, those of the $KNCS$ are bounded in each particular case. This limitation is felt from Eq. (8) that requires c_{Kj} not be zeros. Yet, the c_{Kj} given by Eq. (7) would vanish if the sum over m diverges. The constraint for the existence of $KNCS$'s, i.e. for c_{Kj} not to be zeros, is thus imposed simultaneously on ξ, f and K so that

$$\lim_{m \to \infty} \left\{ |\xi|^{2m} \left[(mK + j)! |f(mK + j)(!)^K|^2 \right]^{-1} \right\} = 0. \quad (9)$$

The importance of this constraint will be seen in the next section when the specific nonlinear function f is addressed.

For a given K the eigenvalue ξ is K-degenerate. The K corresponding eigenfunctions $|\xi; Kj, f\rangle$ with $j = 0, 1, ..., K - 1$ are orthogonal to each other,

$$\langle \xi; Kj, f| \xi; Kj', f\rangle = \delta_{jj'}, \quad (10)$$

as easily verified from the expansion (8). However, with distinct eigenvalues ξ and $\xi' \neq \xi$,

$$\langle \xi; Kj, f| \xi'; Kj, f\rangle = \frac{c_{Kj}(|\xi'|^2)c_{Kj}(|\xi|^2)}{c_{Kj}^2((\xi')^*\xi)} \neq 0. \quad (11)$$

Because of the non-orthogonality (11), the $KNCS$'s constitute an overcomplete set with the following resolution of unity

$$\int \frac{d^2\xi}{\pi} \sum_{j=0}^{K-1} |\xi; Kj, f\rangle \langle \xi; Kj, f| = 1. \quad (12)$$

This section is ended by an interesting observation that any state $|\xi; Kj, f\rangle$ can be decomposed into a linear superposition of K states $|\xi_{j'}; 10, f\rangle$. Namely,

$$|\xi; Kj, f\rangle = \sum_{j'=0}^{K-1} \zeta_{jj'} |\xi_{j'}; 10, f\rangle, \quad (13)$$

with

$$\xi_{j'} = \xi^{1/K} \exp\left(\frac{2\pi ij'}{K}\right) \quad (14)$$

and

$$\zeta_{jj'} = \frac{\xi^{-j/K}}{K} \frac{c_{Kj}(|\xi|^2)}{c_{10}(|\xi|^{2/K})} \exp\left(-\frac{2\pi ijj'}{K}\right). \quad (15)$$

The verification is straightforward by substituting Eqs. (8), (14) and (15) into the r.h.s. of Eq. (13) with subsequent use of the identities

$$\sum_{q=0}^{P-1} \exp\left[\frac{2\pi i}{P}(l - l')q\right] = P\delta_{ll'} \quad (16)$$

and

$$\sum_{n=0}^{\infty} b_n |n\rangle \equiv \sum_{q=0}^{P-1} \sum_{m=0}^{\infty} b_{mP+q} |mP + q\rangle \quad (17)$$

for arbitrary coefficients b_n and integer P.

III. PHYSICAL REALIZATION

Motivated by the physical scheme proposed in [11] we consider a single two-level ion trapped by a harmonic potential $V = kx^2/2$ with k the trapping force and x the ion's center-of-mass position. In the quantized regime the ion vibrates around $x = 0$ with frequency $\nu = \sqrt{k/M}$, M the ion mass. As a whole, the ion Hamiltonian is ($\hbar = c = 1$ throughout)

$$H_0 = \Delta\sigma_3 + \nu a^+ a \quad (18)$$

where Δ is the energy gap between the two electronic levels of the ion, a is the bosonic annihilation operator of a quantum of the quantized vibration of the ion and, σ_3 together with $\sigma_\pm$ are the pseudospin-$\frac{1}{2}$ operators satisfying the commutation relations

$$[\sigma_3, \sigma_\pm] = \pm\sigma_\pm, \quad [\sigma_+, \sigma_-] = 2\sigma_3. \quad (19)$$

By controlling the trapping potential the vibration frequency ν can be made large enough for the sidebands due to the ion quantized motion to be well-resolved. Next, the trapped ion is manipulated by laser beams which couple the ion's electronic to its vibrational degrees of freedom via the light-matter interaction Hamiltonian

$$H_{int} = \sum_{l=1}^{L} \Omega_l \exp\left(\omega_l t + \varphi_l\right) g_l(\widehat{x})\sigma_- + \text{ h.c.} \quad (20)$$

In Eq. (20) L is the number of driving lasers, Ω_l the pure electronic transition Rabi frequencies, ω_l (φ_l) the laser frequencies (phases) and $g_l(\widehat{x})$ the laser spatial profile acting on the ion through its position operator

$$\widehat{x} = \frac{1}{\sqrt{2M\nu}} \left(a^+ + a\right). \quad (21)$$

For traveling waves

$$g_l(\widehat{x}) = \exp\left(\frac{-2\pi i\widehat{x}}{\lambda_l}\right) = \exp\left[-i\eta\left(a^+ + a\right)\right] \quad (22)$$

with λ_l the laser wavelengths and $\eta \simeq \eta_l = 2\pi/(\lambda_l\sqrt{2M\nu})$, the Lamb-Dicke parameter. In the resolved sideband limit the lasers can be tuned so as

$$\omega_l = \Delta + n_l\nu \quad (23)$$

where $n_l = 1, 2, ...$ ($n_l = -1, -2, ...$) imply blue (red) detuning while resonant tuning corresponds to $n_l = 0$. In the interaction representation associated with $\mathcal{H}_0 = H_0$ the laser-driven trapped ion is described by the total Hamiltonian

$$\mathcal{H} = \mathcal{H}_0 + \mathcal{H}_{int} \quad (24)$$

with

$$\mathcal{H}_{int} = \exp\left(iH_0 t\right) H_{int} \exp(-iH_0 t). \quad (25)$$

2

Putting Eqs. (18) and (20) into the r.h.s. of Eq. (25) with use of the Baker-Hausdorff identity and the relations (19) yields

$$\mathcal{H}_{int} = F\sigma_- + \sigma_+ F^+ \qquad (26)$$

with F given by

$$F \equiv F\left(\eta, \widehat{n}, a^+, a\right) =$$
$$\exp(-\frac{\eta^2}{2}) \sum_{l=1}^{L} \left\{ (-i\eta)^{|n_l|}\Omega_l \ (a^+)^{(|n_l|-n_l)/2} \right.$$
$$\left. \left[\sum_{m=0}^{\infty} \frac{(-\eta^2)^m \widehat{n}!}{(m+|n_l|)!m!(\widehat{n}-m)!} \right] a^{(|n_l|+n_l)/2} \right\}. \quad (27)$$

In deriving Eq. (27) terms oscillating with frequencies $m\nu$ ($m \neq 0$) were omitted since those average to zero in the resolved sideband limit we are interested in.

The system state $\Psi(t)$ evolves in time following the equation

$$i\frac{d\Psi}{dt} = \mathcal{H}_{int}\Psi. \qquad (28)$$

We look for long-term nontrivial steady states Ψ_S in which the internal and external degrees of freedom of the ion become decoupled, i.e.

$$\mathcal{H}_{int}\Psi_S = 0. \qquad (29)$$

Such nontrivial solutions would be either $|\uparrow\rangle|\xi\rangle$ or $|\downarrow\rangle|\xi\rangle$ where $|\uparrow\rangle$ ($|\downarrow\rangle$) is the electronic excited (ground) state and $|\xi\rangle$ describes the vibrational state. The state $|\uparrow\rangle|\xi\rangle$ is unstable due to spontaneous emission which was not treated explicitly here. The remaining "dark" state $|\downarrow\rangle|\xi\rangle$ is stable with $|\xi\rangle$ satisfying the condition

$$F^+|\xi\rangle = 0. \qquad (30)$$

Similar "dark" states have been obtained as an ansatz of master equations with spontaneous emission included [16,11]. From Eqs. (28) and (30) it follows that the nontrivial state $|\xi\rangle$ exists iff there are at least two driving lasers. For generality, let there be P (Q) red-detuned (blue-detuned) laser beams and a single resonant one. Then, the coefficients of the expansion of $|\xi\rangle$ in the Fock space,

$$|\xi\rangle = \sum_{l=0}^{\infty} C_l |l\rangle, \qquad (31)$$

are recurrent as

$$\sum_{p=1}^{P} (i\eta)^{|n_p|} \Omega_p e^{-i\varphi_p} \sqrt{\frac{l!}{(l+|n_p|)!}} L_l^{|n_p|}(\eta^2) C_{l+|n_p|}$$

$$+\sum_{q=1}^{Q} \theta\left(l-n_q\right)(i\eta)^{n_q}\Omega_q e^{-i\varphi_q}\sqrt{\frac{(l-n_q)!}{l!}}L_{l-n_q}^{n_q}(\eta^2)C_{l-n_q}$$

$$+ \Omega_0 e^{-i\varphi_0} L_l^0(\eta^2) C_l = 0 \qquad (32)$$

where $\theta(x)$ is the step function and $L_n^m(x)$ the n-th generalized Laguerre polynomial in x for parameter m.

For the purpose of generating the KNCS defined in the preceding section we restrict to $P = 1$, $n_{p=1} = -K$ and $Q = 0$ and get from Eq. (32)

$$C_{l+K} = -\frac{e^{i\varphi}\Omega_0\sqrt{(l+K)!}L_l^0(\eta^2)}{(i\eta)^K\Omega_1\sqrt{l!}L_l^K(\eta^2)}C_l \qquad (33)$$

with $\varphi = \varphi_1 - \varphi_0$. Comparing Eqs. (33) and (4) indicates that $|\xi\rangle$ obeying Eq. (30) is a KNCS with the physical controllable eigenvalue

$$\xi = -\frac{e^{i\varphi}\Omega_0}{(i\eta)^K\Omega_1} \qquad (34)$$

and the specific, also controllable, nonlinear function

$$f\left(\widehat{n} + K\right) = \frac{\widehat{n}!L_{\underset{n}{K}}(\eta^2)}{(\widehat{n}+K)!L_{\underset{n}{0}}(\eta^2)}. \qquad (35)$$

In the next section the number distribution, squeezing and antibunching of the KNCS with the specific ξ and f given above will be studied in detail. To that aim let us define the function

$$g_{Kj}(n,l) = \frac{\xi^{n+l/K}}{\sqrt{(nK+j+l)!}\ f(nK+j+l)(!)^K} \qquad (36)$$

in terms of which

$$|\xi; Kj, f\rangle = \frac{\sum_{n=0}^{\infty} g_{Kj}(n,0)\,|nK+j\rangle}{\sqrt{\sum_{m=0}^{\infty}|g_{Kj}(m,0)|^2}}. \qquad (37)$$

It is worth to emphasize that the KNCS does not exist for arbitrary control parameters η and ξ. For a fixed trapping potential characterized by η the amplitudes (phases are not sensitive in this scheme with $Q = 0$ and $P = 1$) of the driving fields must be chosen such that the constraint (9) is met, i.e. $\lim_{n\to\infty}|g_{Kj}(n,0)|^2 = 0$. Figure 1, $\log(|g_{Kj}(n,0)|^2)$ versus n, shows opposite limiting behaviors for the same value of η but different $|\xi|$. In general, there is a critical $|\xi_c|$ above which the KNCS vanishes. This critical $|\xi_c|$ depends strongly on both η and K but not on j. Phase diagrams for the existence domain of the KNCS are drawn in Fig. 2 in the $(\eta,|\xi|)$-plane for $K = 1, 2$ and 3. These diagrams guide the appropriate experimental choice of the control parameters to observe the KNCS with a concrete K.

IV. NONCLASSICAL EFFECTS

A. Multi-peaked number distribution

The probability of finding n quanta in the KNCS, i.e. its number distribution, is given by

$$P_{Kj}(n) = \frac{I(\frac{n-j}{K})}{\sum_{m=0}^{\infty} |g_{Kj}(m,0)|^2} \left| g_{Kj}(\frac{n-j}{K}, 0) \right|^2 \quad (38)$$

where $I(x)$ equals x if x is a non-negative integer and zero otherwise. The tortuous shape in Fig. 1 gives rise to a multi-peaked structure of $P_{Kj}(n)$ as depicted in Fig. 3 in the case $K = 1$, $j = 0$. The multi-peaked distribution is very peculiar compared to the Poisson's in the usual CS. However, multiple peaking disappears in the Lamb-Dicke limit $\eta \ll 1$ in which $|g_{Kj}(n,0)|$ varies monotonically (not tortuously) for increasing n having only one peak at some value $n > 0$ and then decreasing quickly. The developing from single- to multi-peaked structure as η increases can be called self-splitting [11] which would bring about abundant nonclassical phenomena including quantum interferences if the peaks are located nearby and comparable in heights. As for higher orders K, unexpectedly, the self-splitting tends to be less pronounced as seen from Fig. 4. Besides getting less tortuous, the more important fact is that the curve decreases much faster for higher K. Hence, for $K > 1$ the η-governed self-splitting is negligible physically. Instead, for $K > 1$, another kind of splitting, the K-governed one, appears independent of the Lamb-Dicke parameter. This is dictated by the presence of $I(\frac{n-j}{K})$ in Eq. (38). Namely, for $K > 1$ the number distribution "oscillates" with "period" K and its "phase" is j-dependent. The P_{30}, P_{31} and P_{32} plotted in Fig. 5 illustrate that, in the state $|\xi; 30, f\rangle$ ($|\xi; 31, f\rangle$; $|\xi; 32, f\rangle$), finite is only the probability of finding $3, 6, 9, ...$ $(4, 7, 10, ...; 5, 8, 11, ...)$ quanta. Generally speaking, only a number of quanta equal to a multiple K plus j ($j = 0$, $1, ..., K - 1$) can be found in the state $|\xi; Kj, f\rangle$. Given K each j-state occupies its own subspace and all the different j-states fill the entire Fock space. Therefore, the notion "number-parity" might be introduced. A state is said to have a number-parity Kj if it contains only $nK + j$ ($n = 0, 1, 2, ...$) quanta. For $K = 2$ the parity gets its intuitive meaning: the state $|\xi; 20, f\rangle$ ($|\xi; 21, f\rangle$) contains only even (odd) numbers of quanta and it can be referred to as even (odd) NCS [21,22]. This evenness (oddness) is also clear from the view point of the decomposition (13) according to which

$$|\xi; 20, f\rangle = \zeta_{00} |\xi_0; 10, f\rangle + \zeta_{01} |\xi_1; 10, f\rangle, \quad (39)$$

$$|\xi; 21, f\rangle = \zeta_{10} |\xi_0; 10, f\rangle + \zeta_{11} |\xi_1; 10, f\rangle. \quad (40)$$

By virtue of Eqs. (14) and (15), $\xi_0 = -\xi_1$ and $\zeta_{00} = \zeta_{01} = \zeta_{10} = -\zeta_{11}$. These mean that the combination in Eq. (39) is symmetric leading to evenness, while that in Eq. (40) is anti-symmetric leading to oddness.

Because the $\mathcal{H}_{int}$ determined in Eqs. (26) and (27) for $P = 1$, $n_{p=1} = -K$, $Q = 0$ creates/annihilates K quanta at a time the number-parity is conserved. If initially the vibration quanta are in a Fock state $|m\rangle$ then the steady state Ψ_S will have number-parity Kj with j the remainder of m divided by K. By sideband cooling modern techniques the fundamental limit has been reached in which the ion vibrational motion can be kept to zero-point energy 98% (92%) of the time in 1D (3D) [20]. If such a ground state is further manipulated by lasers as proposed above, then the state $|\xi; K0, f\rangle$ will be realized. If, the initial quanta are prepared in a CS $|\alpha\rangle$ then the eventual state will be a mixed state with weighted j-components

$$\Psi_S = \Psi_K^{mix} = \sum_{j=0}^{K-1} \beta_{Kj} |\xi; Kj, f\rangle. \quad (41)$$

Assuming the weights β_{Kj} be as in the CS,

$$\beta_{Kj} = \exp\left(-\frac{|\alpha|^2}{2}\right) \sqrt{\sum_{m=0}^{\infty} \frac{|\alpha|^{2(mK+j)}}{(mK+j)!}}, \quad (42)$$

the number distribution P_K^{mix} of the mixed state Ψ_K^{mix} will differ noticeably under two situations: $|\alpha| < K$ and $|\alpha| \geq K$. For $|\alpha| < K$ the β_{Kj} are scattered whereas for $|\alpha| \geq K$ they get equal, $\beta_{Kj} = 1/\sqrt{K}$, for all j reducing P_K^{mix} simply to

$$P_K^{mix}(n) = \frac{1}{K} \left(\sum_{j=0}^{K-1} \sqrt{P_{Kj}(n)} \right)^2 \quad (43)$$

with $P_{Kj}(n)$ given in Eq. (38), independent of α. Figure 6 addresses the above-said issue for $K = 6$ and several values of $|\alpha|$. The $P_K^{mix}(n)$ spans the whole Fock space with different α-dependent profiles. This is of course subject to experimental checking to which extent the assumption (42) is valid.

B. Squeezing and antibunching

In the small η limit the $K = 1$ NCS exhibits a single-peaked number distribution that may be super- or sub-poissonian. So happens as well for the envelope of the $K > 1$ NCS distribution. Sub-poisson distribution featuring antibunching occurs whenever the Mandel parameter,

$$M = \frac{\langle \hat{n}^2 \rangle}{\langle \hat{n} \rangle} - \langle \hat{n} \rangle, \quad (44)$$

is less than 1. We shall also examine amplitude-quadrature squeezing of the ion center-of-mass position operator (in units of $(2M\nu)^{-1/2}$, for convenience) $\overline{x} = a^+ + a$ by calculating its variance $\left\langle (\Delta \overline{x})^2 \right\rangle = 1 + 2S$ with S given by

$$S = \langle \hat{n} \rangle + \Re \langle a^2 \rangle - 2\Re^2 \langle a \rangle. \quad (45)$$

The KNCS gets squeezed in $\overline{x}$ if $-0.5 \leq S < 0$. In terms of the functions $g_{Kj}(m, l)$ defined in Eq. (36)

4

$$\langle a^l \rangle_{Kj} = \frac{\sum_{m=0}^{\infty} \left[\sqrt{\frac{(mK+j+l)!}{(mK+j)!}} g^*_{Kj}(m,0) g_{Kj}(m,l) \right]}{\sum_{m=0}^{\infty} |g_{Kj}(m,0)|^2},$$

(46)

$$\langle \hat{n}^l \rangle_{Kj} = \frac{\sum_{m=0}^{\infty} \left[(mK+j)^l |g_{Kj}(m,0)|^2 \right]}{\sum_{m=0}^{\infty} |g_{Kj}(m,0)|^2}.$$

(47)

The analytic expressions of M and S are readily obtained using Eqs. (46) and (47) in (44) and (45). For $K = 1$ it is found that $S > 0$, i.e. no squeezing, but M decreases from 1 for increasing $|\xi|$ (see Fig. 7), i.e. antibunching. Such effects are opposed to the usual CS for which $S = 0$ and $M = 1$ for all $|\xi|$. As was well-known, for $f \equiv 1$ the state $|\xi; 20, 1\rangle$ possesses squeezing but no antibunching whereas the state $|\xi; 21, 1\rangle$ does the inverse: antibunching but no squeezing. The KNCS with the specific nonlinear function f given by Eq. (35) causes curious changes. The state $|\xi; 20, f\rangle$ is squeezed in a rather narrow range of small values of $|\xi|$ (see Fig. 8a) and turns from super- to sub-poisson's as $|\xi|$ increases (see Fig. 8b). As for the state $|\xi; 21, f\rangle$ it remains unsqueezed but antibunched for all $|\xi|$ as were no affect of f. For $K = 3$, the state $|\xi; 30, f\rangle$ behaves qualitatively like the state $|\xi; 20, f\rangle$ does. The state $|\xi; 31, f\rangle$ is non-squeezed but, most curiously, its number distribution crosses 1 twice (see Fig. 9). At small values of $|\xi|$, the Mandel parameter M_{31} is less than 1. It crosses 1 becoming super-poissonian but, after reaching a maximum, drops back below 1 and remains there being sub-poissonian in the whole high-value side of $|\xi|$. Finally, no squeezing and permanent antibunching are found in the state $|\xi; 32, f\rangle$.

V. CONCLUSION

We have introduced the K-quantum nonlinear coherent state. For a given K there are K mutually orthogonal substates belonging to the same eigenvalue. Each of such substates can be decomposed into a linear combination of K usual nonlinear coherent states with correlated eigenvalues and weights determined respectively by Eqs. (14) and (15). States with the same K and j but belonging to two different eigenvalues ξ and $\xi' \neq \xi$ are however non-orthogonal to each other and, the states with a fixed K and all possible ξ and j are overcomplete. A harmonically trapped two-level ion driven properly by two laser beams, one in resonance with the ion's electronic transition and the other detuned to the Kth lower sideband, is shown to realize the K-quantum nonlinear coherent state in the steady regime for suitably chosen control parameters. These states show up two kinds of multiple self-peaking in their number distribution. One kind is associated with large values of the Lamb-Dicke parameter η but is not pronounced for $K > 1$. The other

kind originates from $K > 1$ independent of η and is manifested in the number distribution that fills the Fock space "periodically" with "period" K, forming a multi-peaked structure. Squeezing and antibunching have been investigated in detail revealing curious features corresponding to the specific nonlinear function $f(\hat{n})$ which is here well-determined in the context of a trapped ion driven by lasers with the certain setup. Another setup of driving lasers, say, with $P = 0$ and $Q = 1$, or whatever else, would lead to another class of states.

[1] R. J. Glauber, Phys. Rev. Lett. **10**, 84 (1963).
[2] E. C. G. Sudarshan, Phys. Rev. Lett. **10**, 277 (1963).
[3] D. Stoler, Phys. Rev. **D 1**, 3217 (1970); **4**, 1935 (1971).
[4] C. K. Hong and L. Mandel, Phys. Rev. **A 32**, 974 (1985).
[5] M. Hillery, Phys. Rev. **A 36**, 3796 (1987); **40**, 3147 (1989).
[6] A. Kumar and P. S. Gupta, Opt. Commun. **136**, 441 (1997); Quantum Semiclass. Opt. **10**, 485 (1998).
[7] Nguyen Ba An and Vo Tinh, Phys. Lett. **A 261**, 34 (1999); **270**, 27 (2000); J. Phys. **A**: Math. Gen. **33**, 2951 (2000).
[8] L. C. Biedenharn, J. Phys. **A**: Math. Gen. **22**, L873 (1989).
[9] A. J. Macfarlane, J. Phys. **A**: Math. Gen. **22**, 4581 (1989).
[10] V. I. Manko, G. Marmo, S. Solimeno, and F. Zaccaria, Int. J. Mod. Phys. **A 8**, 3577 (1993).
[11] R. L. de Mator Filho and W. Vogel, Phys. Rev. **A 54**, 4560 (1996).
[12] V. I. Manko, G. Marmo, E. C. G. Sudarshan, and F. Zaccaria, Physica Scripta **55**, 528 (1997).
[13] B. Roy and P. Roy, J. Opt. **B**: Quantum Semiclass. Opt. **1**, 341 (1999); **2**, 65 (2000).
[14] A. Aniello, V. Manko, G. Marmo, S. Solimeno, and F. Zaccaria, J. Opt. **B**: Quantum Semiclass. Opt. **2,** 718 (2000).
[15] S. Sivakumar, J. Opt. **B:** Quantum Semiclass. Opt. **2,** R61 (2000).
[16] J. I. Cirac, A. S. Rarkins, B. Blatt, and P. Zoller, Phys. Rev. Lett. **70**, 556 (1993).
[17] R. L. de Mator Filho and W. Vogel, Phys. Rev. **A 50**, R1988 (1994); Phys. Rev. Lett. **76**, 608 (1996).
[18] D. M. Meekhof, C. Monroe, B. E. King, W. M. Itano, and D. J. Wineland, Phys. Rev. Lett. **76**, 1796 (1996).
[19] M. Jakov and G. Y. Kryuchkyan, Phys. Rev. **A 61**, 53823 (2000).
[20] C. Monroe, D. M. Meekhof, B. E. King, S. R. Jeffers, W. M. Itano , and D. J. Wineland, Phys. Rev. Lett. **75**, 4011 (1995).

[21] S. Mancini, Phys. Lett. **A 233**, 291 (1997).
[22] B. Roy and P. Roy, Phys. Lett. **A 257**,264 (1999).

FIGURE CAPTIONS

Fig. 1: $\log(|g_{Kj}(n,0)|^2)$ as a function of n for $K = 1$, $j = 0$, $\eta = 0.5$ while a) $|\xi| = 1.2$, a converging case, and b) $|\xi| = 3.2$, a diverging case.

Fig. 2: Phase diagrams in the $(\eta,|\xi|)$-plane for various K whose values are indicated near the curve. The curves, themselves, are the $|\xi_c|$ as a function of η. The corresponding KNCS exists (does not exist) below (above) the curve.

Fig. 3: Number distributions for the states $|\xi; 10, f\rangle$ with $\eta = 0.5$ while a) $|\xi| = 1.5$ and b) $|\xi| = 1.8$, featuring two-peaked structures.

Fig. 4: $\log(|g_{K0}(n,0)/\xi^n|)$ versus n for $\eta = 0.5$ and different orders K indicated near the curve. The curve gets less tortuous and drops much faster for a higher K.

Fig. 5: Number distributions P_{Kj} versus n for $\eta = 0.05$, $|\xi| = 100$, $K = 3$ while a) $j = 0$, b) $j = 1$ and c) $j = 2$, featuring multi-peaked structures.

Fig. 6: Number distributions of the mixed state resulting from an initial coherent state $|\alpha\rangle$ for $K = 6$, $\eta = 0.05$, $|\xi| = 100$ and different values of $|\alpha|$ as indicated. The curve with $|\alpha| = 6$ remains unchanged for $|\alpha| > 6$.

Fig. 7: Mandel parameter against $|\xi|$ for $K = 1$, $j = 0$ and $\eta = 0.05$ showing antibunching as opposed to the case with $f \equiv 1$. Antibunching occurs as well for higher values of η.

Fig. 8: a) Squeezing to non-squeezing and b) super- to sub-poisson's transition as $|\xi|$ increases for the state $|\xi; 20, f\rangle$ with $\eta = 0.05$ (similarly for higher η).

Fig. 9: Mandel parameter as a function of $|\xi|$ for $K = 3$, $j = 1$ and $\eta = 0.05$ (similarly for higher η): the transition from sub-poisson's to super-poisson's and back to sub-poisson's in the course of increasing $|\xi|$.
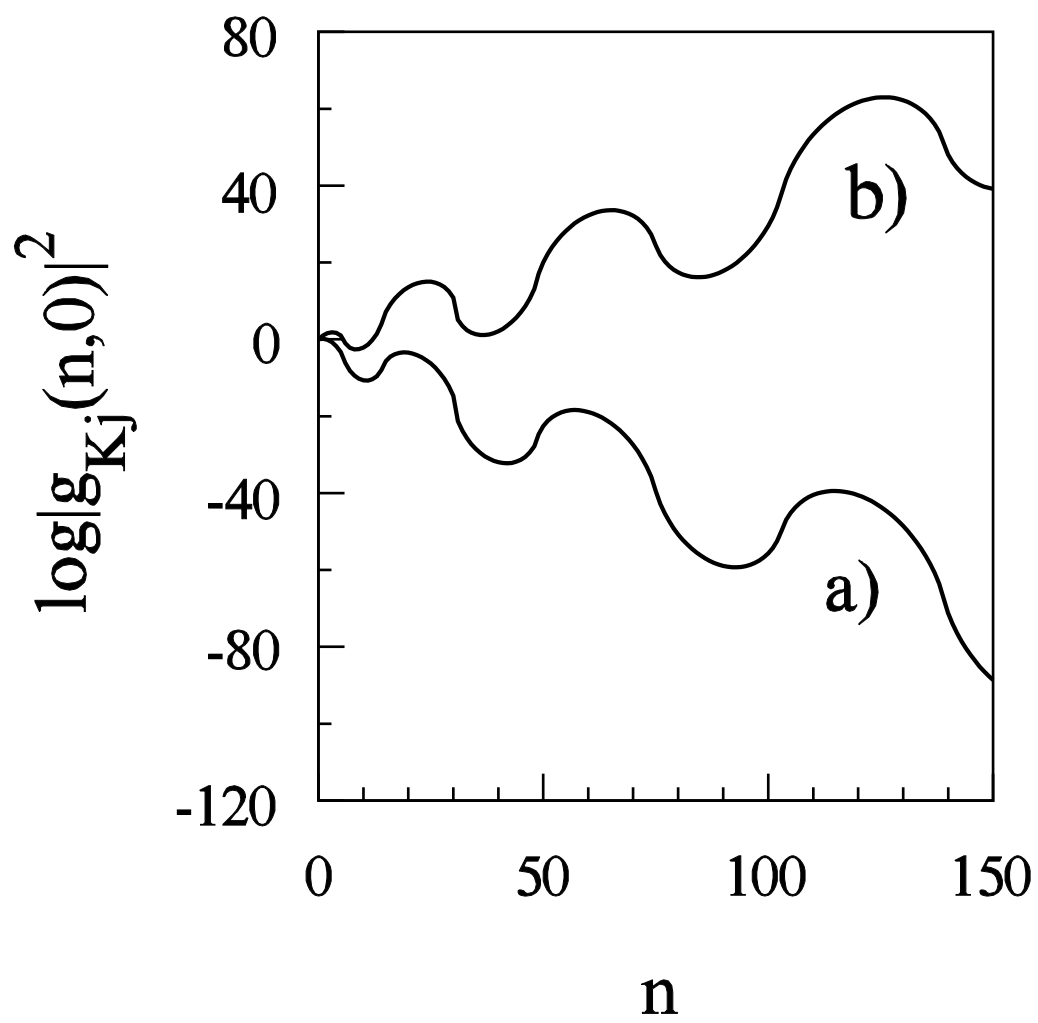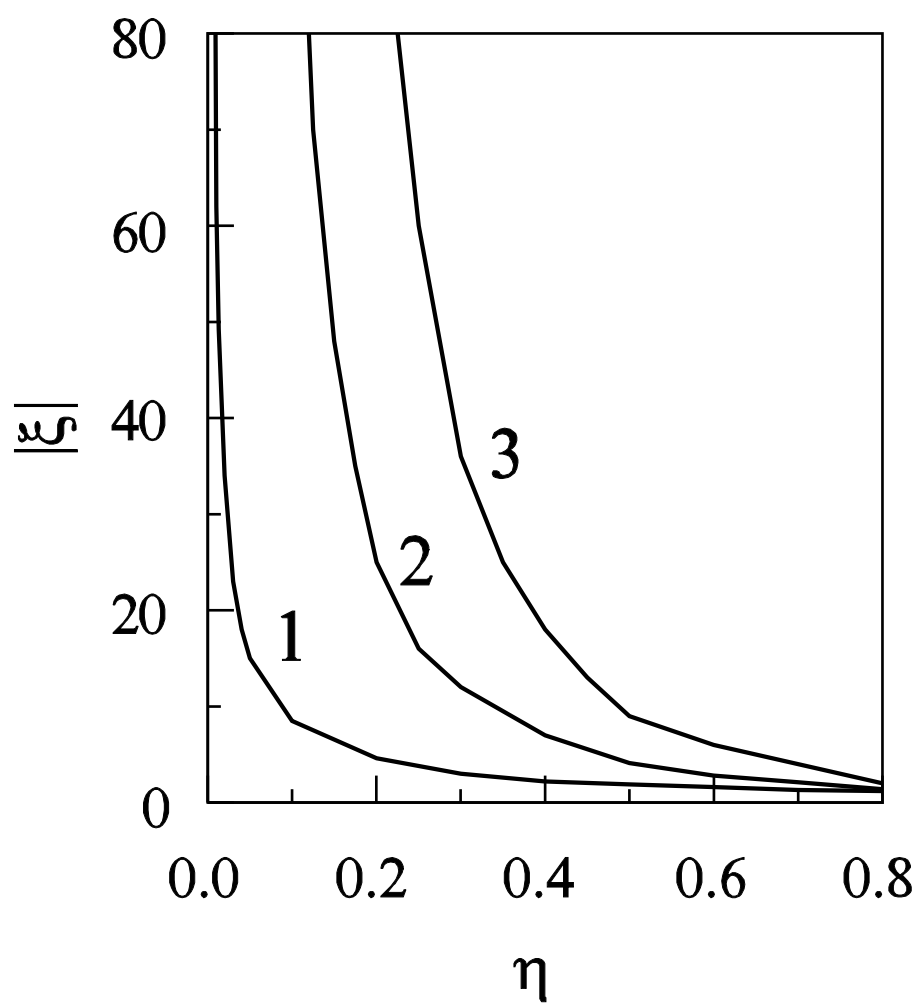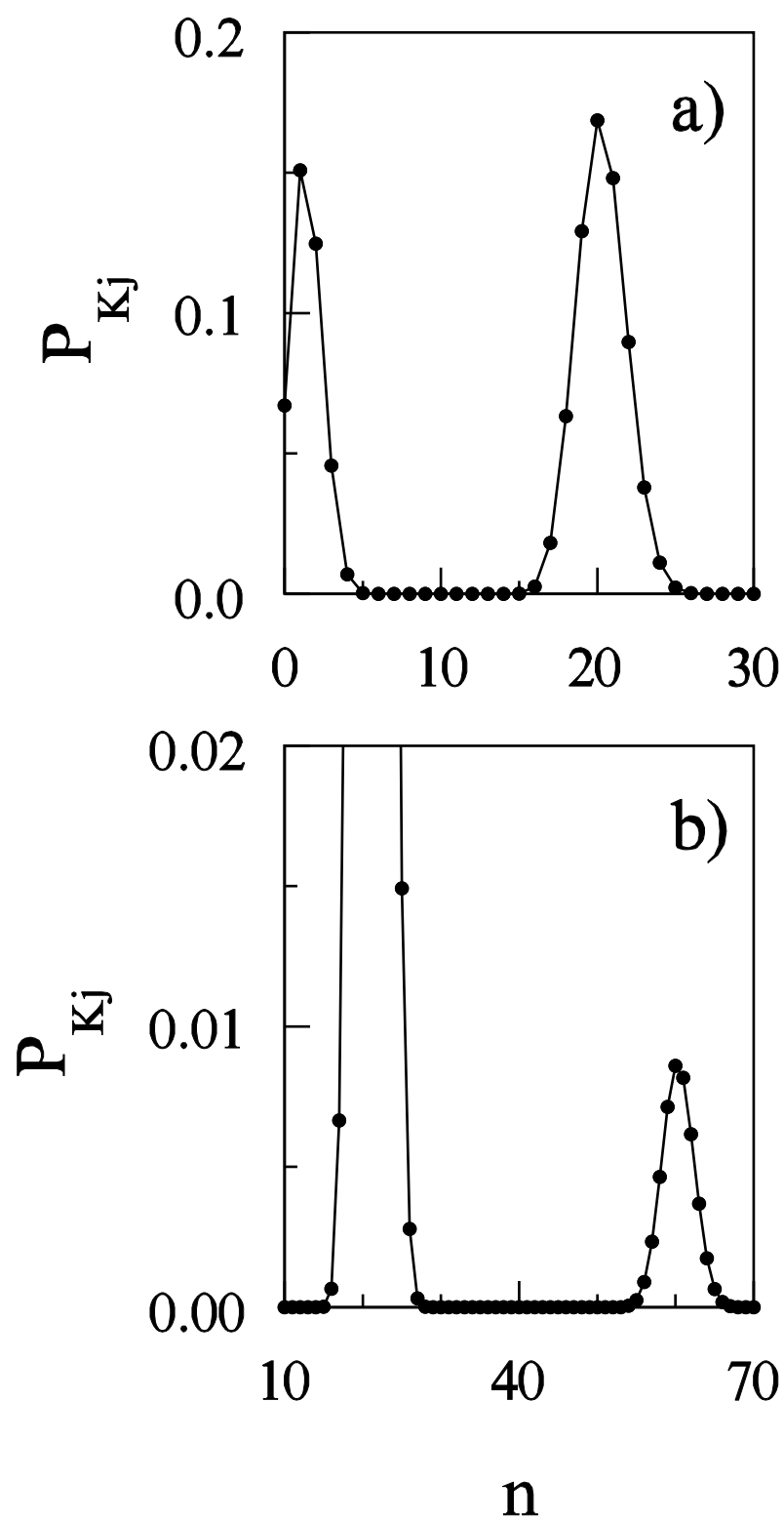
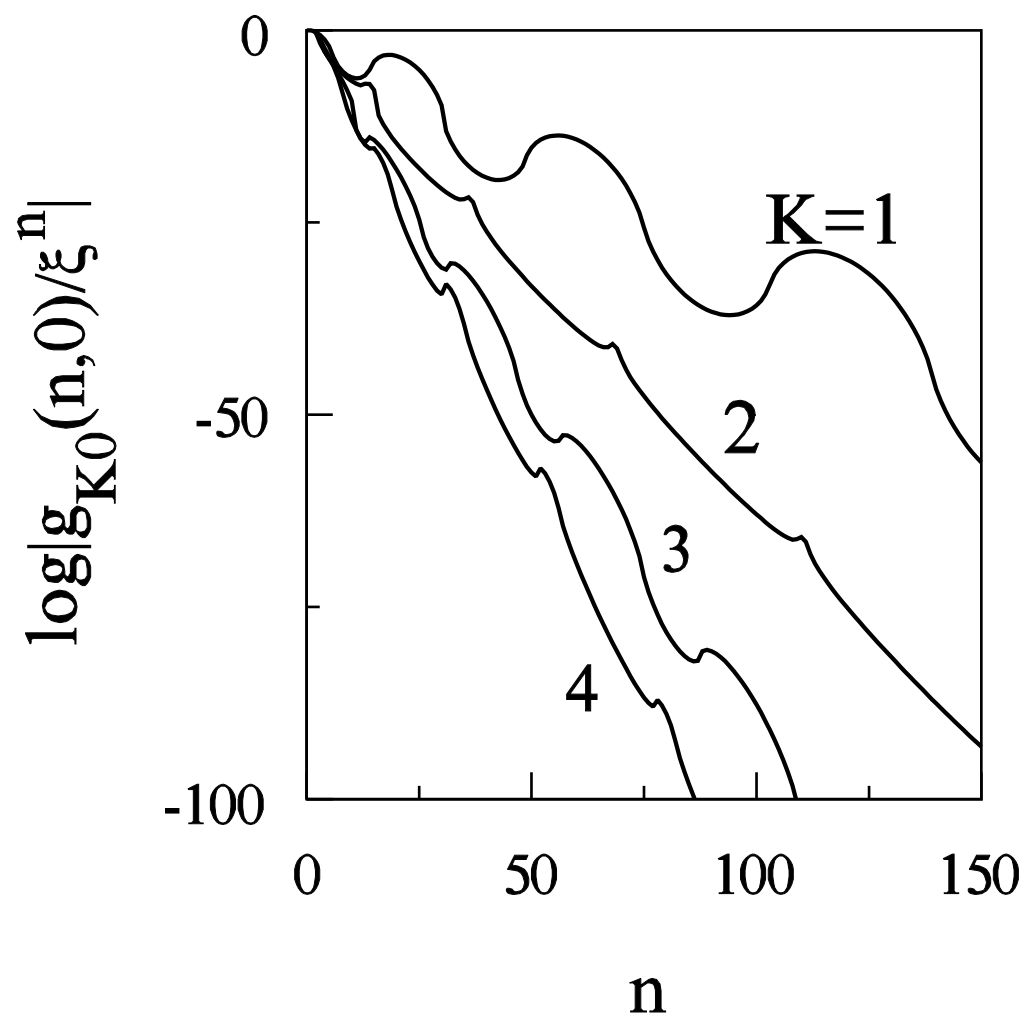Fig.1, Nguyen Ba An

Fig.2, Nguyen Ba An
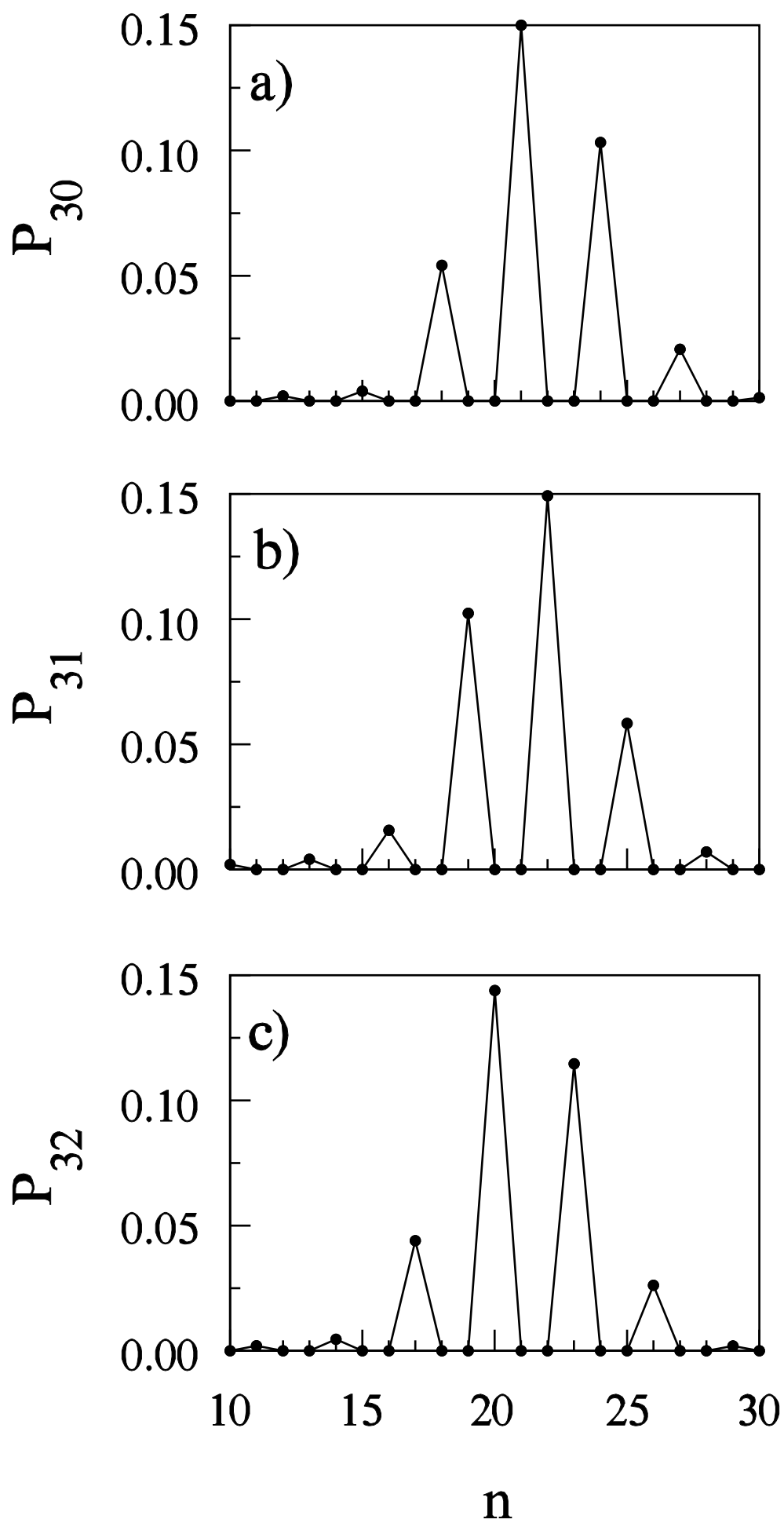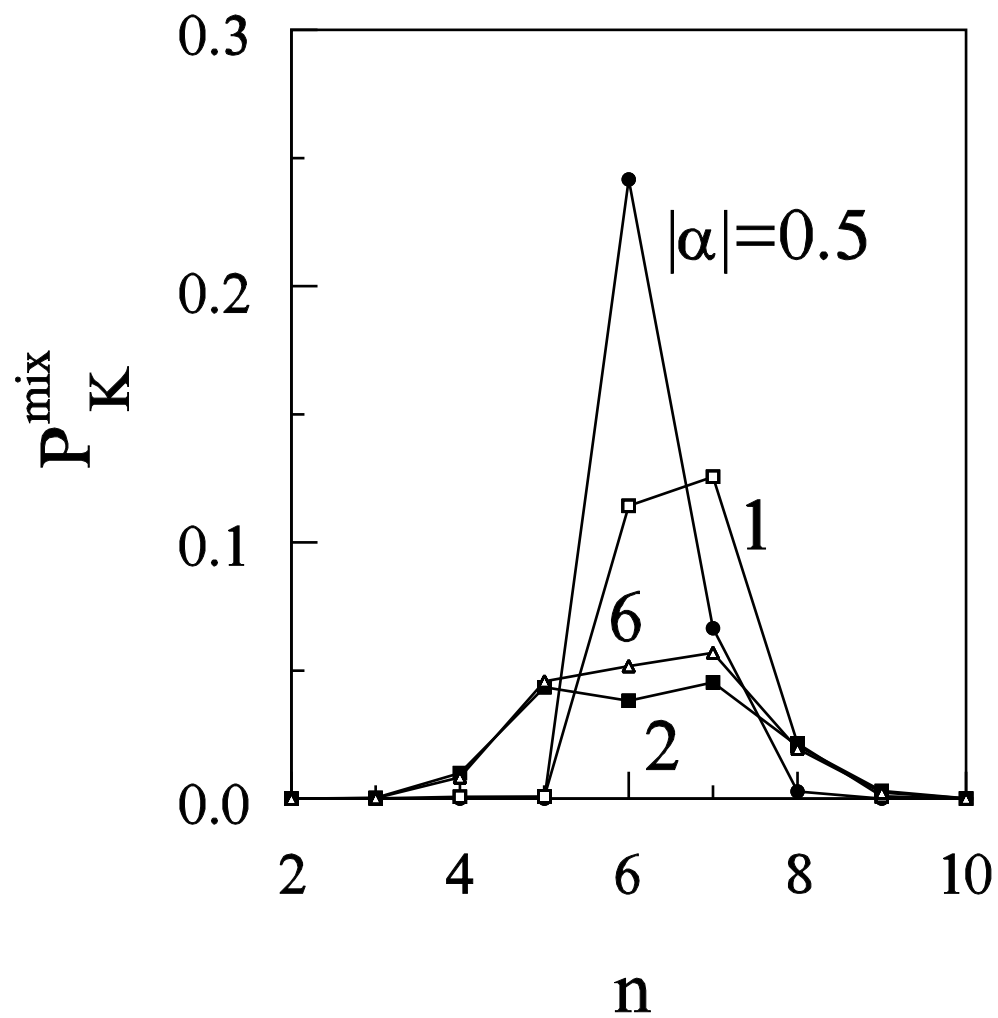
Fig.3, Nguyen Ba An
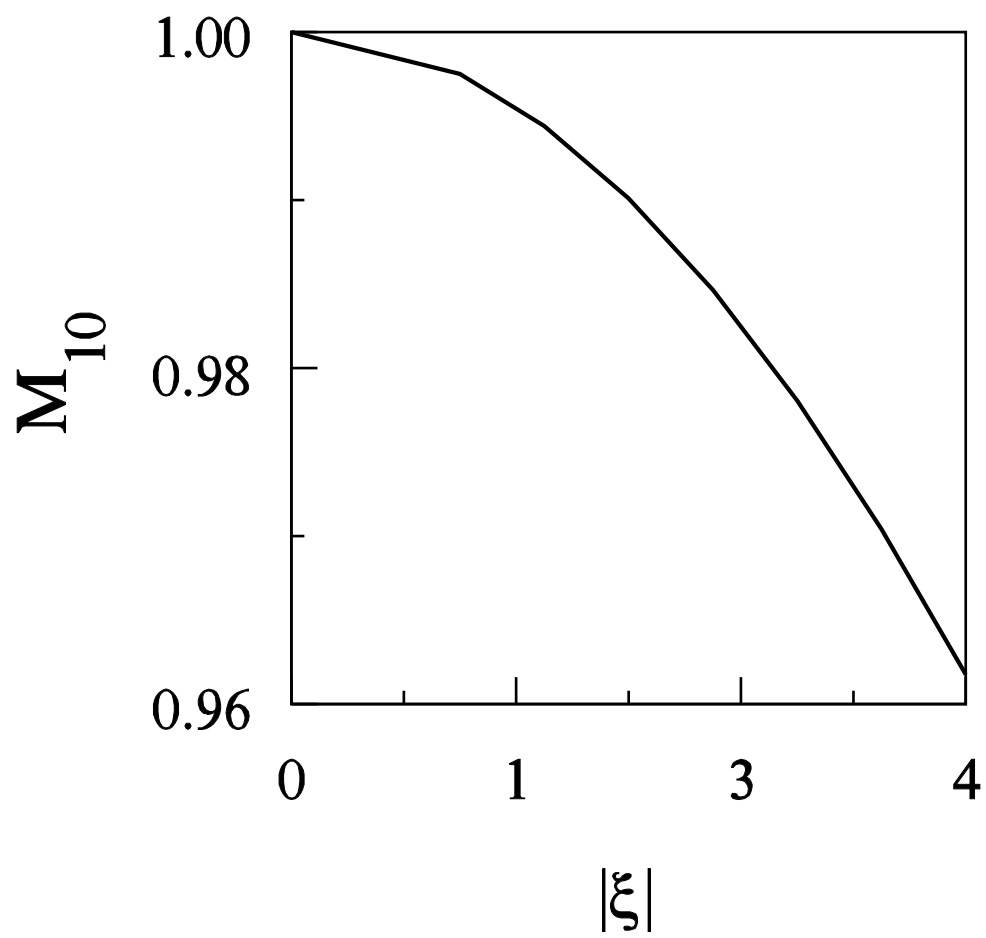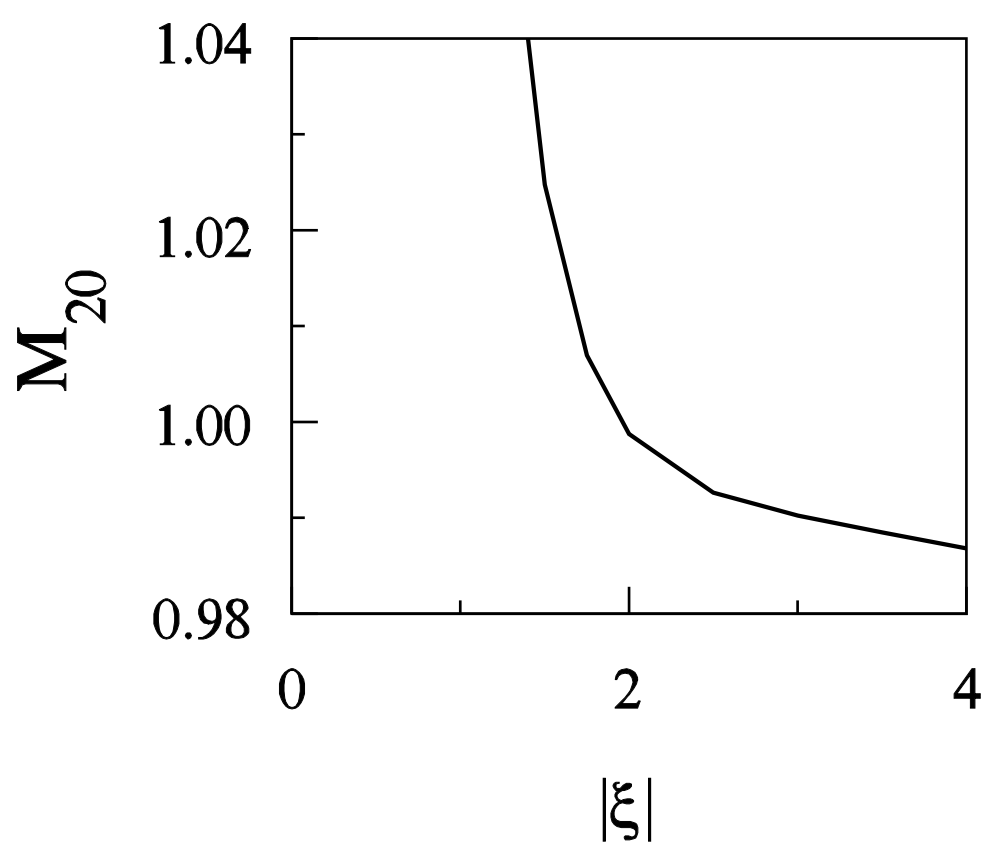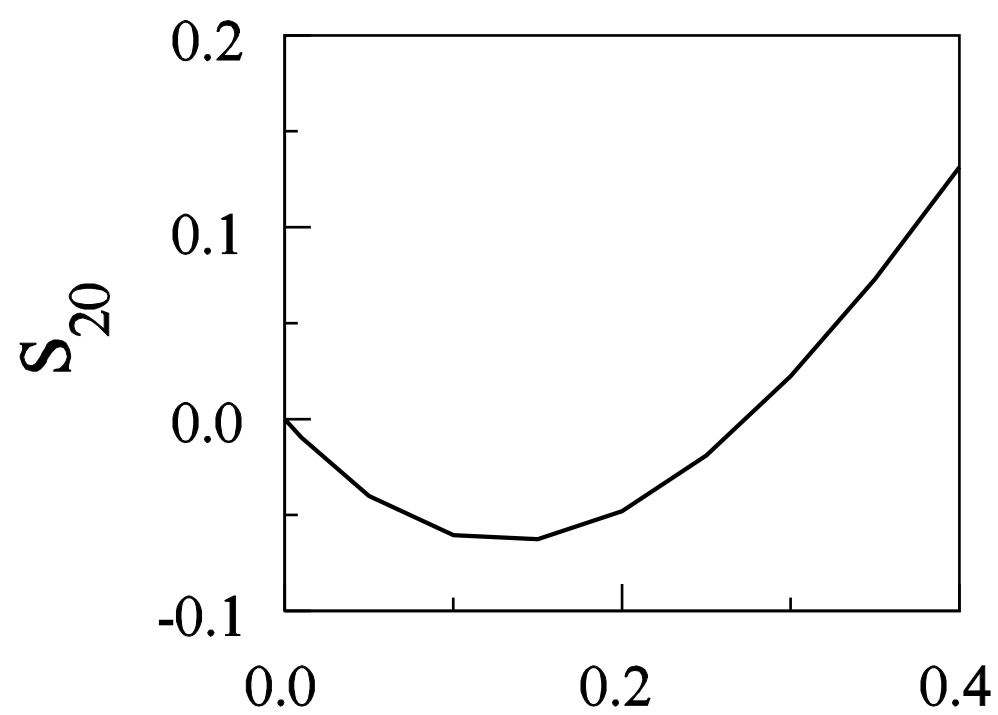
Fig.4, Nguyen Ba An

Fig.5, Nguyen Ba An

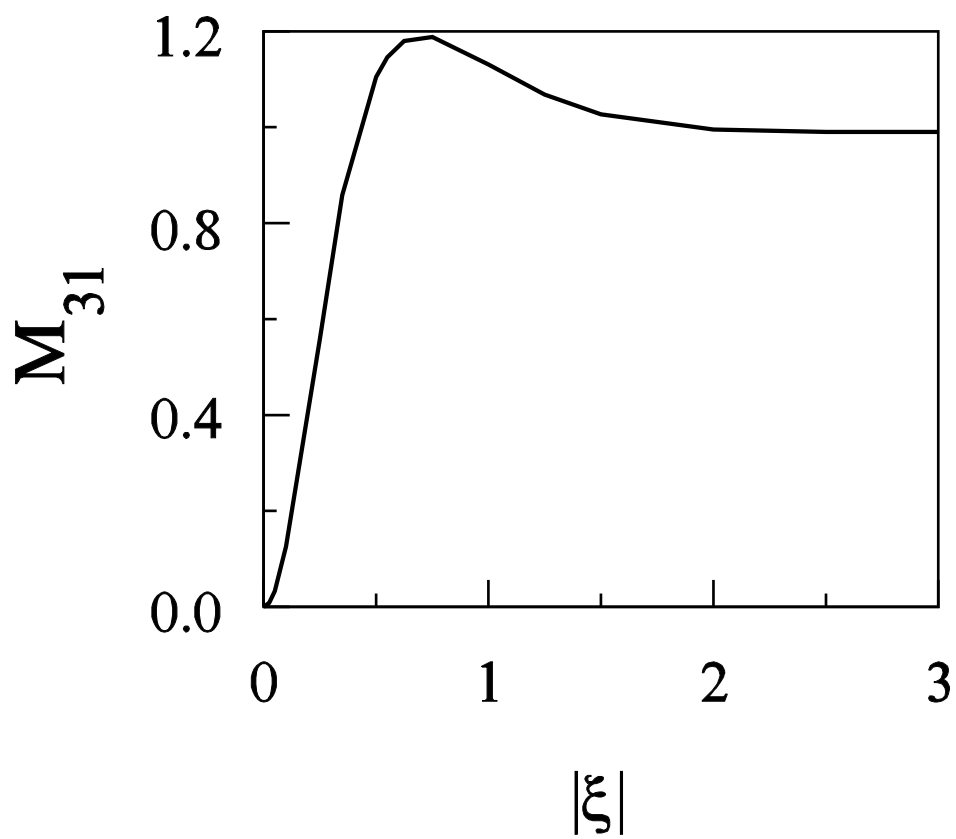Fig.6, Nguyen Ba An

Fig. 7, Nguyen Ba An

Fig. 8, Nguyen Ba An

Fig. 9, Nguyen Ba An